

Spectroscopic Observation of the Dimerization Reactions of the 9-Phenylcarbazole Cation Radical in Acetonitrile

Munetaka Oyama* **and Jun Matsui**

Division of Research Initiatives, International Innovation Center, Kyoto University, Sakyo-ku, Kyoto 606-8501

Received June 19, 2003; E-mail: oyama@iic.kyoto-u.ac.jp

The dimerization reaction processes of the 9-phenylcarbazole cation radical ($PCZ^{\bullet+}$) in acetonitrile (AN) were observed using an electron-transfer stopped-flow method. Although the lifetime of $PCZ^{\bullet+}$ in AN is less than a few hundred milliseconds, the dynamic transformation of the absorption spectra of $PCZ^{\bullet+}$ was successfully observed in AN for the first time with the proposed method. By observing the changes in the absorption spectra in the visible region, the decrease in $PCZ^{\bullet+}$ and the concurrent increase in the dimer cation radical were observed with isosbestic points. In addition, in the presence of neutral PCZ, the acceleration of the dimerization of $PCZ^{\bullet+}$ was clearly confirmed. Consequently, in the presence of PCZ, the rate law was determined to be $-d[PCZ^{\bullet+}]/dt = 3Kk'[PCZ^{\bullet+}]^2[PCZ]$, where $3Kk'$ is 1.4×10^9 M^{-2} s^{-1}. This means that the reaction mechanism involves a two-step interaction with the catalytic effect of neutral PCZ. Although the difference in the reactivity had already been known between $PCZ^{\bullet+}$ and the triphenylamine cation radical, the reaction mechanism has been clarified to be different in both cases.

The mechanisms of the electro-oxidative dimerization reactions in aprotic solvents have been studied extensively, e.g., as summarized in a review by Schmittel and Burghart.[1] Depending on the identity of the cation radicals, cation radical–substrate coupling (RSC) or the cation radical–cation radical coupling (RRC) mechanism has been applied to explain the electrochemical results. However, there is a mechanistic uncertainty between both mechanisms.[1] Although the RRC mechanism was actually applicable for the dimerization of aromatic amine derivative cation radicals in spite of a charge repulsion,[2–4] the RSC mechanism was verified in some other cases.[5–7] In particular, for the latter mechanism, careful mechanistic discriminations involving the precursor molecules should be necessary in an electrochemical analysis, because the precursor molecules surely exist in the bulk solution to produce the cation radicals.

Recently, we proposed an electron-transfer stopped-flow (ETSF) method,[4] and utilized it for revealing various complex aspects of the reactions of aromatic amine cation radicals due to the presence of precursor molecules.[8–12] In the ETSF method, it is characteristic that the thermodynamically favorable electron transfer reactions between long-lived cation radicals and neutral molecules are utilized to form unstable cation radicals.[4] Although the ETSF method is not an electrochemical method, it has great advantages in that the reaction processes of cation radicals can be analyzed in homogeneous solutions under rigid control of the concentration of the coexisting precursor molecules.

The mechanistic findings achieved by the ETSF method can be summarized as follows:

1) The dimerization reaction of methyldiphenylamine and diphenylamine cation radicals in acetonitrile (AN) proceeds via the RRC mechanism. The precursor molecules affect only the equilibria involving the oxidation states of the dimer benzidines.[4]

2) The dimerization reaction of the 4-bromo-*N*,*N*-dimethylaniline cation radical proceeds via the RRS to form the tetramethylbenzidine dication when the cation radical is quantitatively formed without a precursor. In the presence of precursor molecules, the tetramethylbenzidine cation radical is formed via nucleophilic attack of the precursor on the cation radical, i.e., the RSC mechanism, with high reactivity.[10]

3) The decay reaction of the *N*,*N*-dimethyl-*p*-toluidine cation radical proceeds via an acid–base reaction between the cation radical and the precursor, which is similar to the RSC mechanism, but actually via a radical–radical coupling of the H^+-extracted form of the cation radical.[10,11] This mechanism was also verified using electrochemical methods.[13]

4) In the reaction of the 1-aminopyrene cation radical, the precursor molecule was found to promote the rate of the initial reaction of the polymerization. Mechanistically, the first reaction between the cation radical with the precursor is in equilibrium, and the second step involving another cation radical is the rate-determining reaction.[12]

In the present paper, as an example of the spectroscopic detection of short-lived cation radicals and clear-cut reaction analysis involving the precursor molecules, we would like to present how we could observe the dimerization reaction of the 9-carbazole cation radical in AN using the ETSF method.

The reaction pathways of various carbazole cation radicals in AN were thoroughly investigated by Nelson and co-workers.[14,15] Among the carbazole derivatives studied, the reaction of 9-phenylcarbazole cation radicals ($PCZ^{\bullet+}$), for which the formation of the dimer (3,3′-dimer) is known,[15] would be of interest in relation to the reaction of the triphenylamine cation radical ($TPA^{\bullet+}$). The structures of the compounds are shown in Chart 1. $PCZ^{\bullet+}$ has a planer carbazole ring, whereas all of the phenyl groups of $TPA^{\bullet+}$ are twisted.

Reflecting this difference, a much faster (ca. 10^4 times faster)

Published on the web May 6, 2004; DOI 10.1246/bcsj.77.953

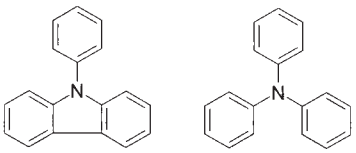

PCZ TPA

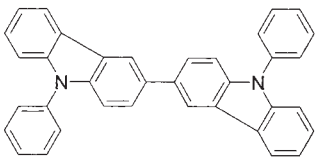

3, 3'-Dimer

Chart 1.

dimerization reaction rate of $PCZ^{\bullet+}$ has been reported for $PCZ^{\bullet+}$ compared with that of $TPA^{\bullet+}$; the bimolecular coupling rate constant was estimated to be 9 ($\pm$ 6) $\times$ 10^7 M^{-1} s^{-1} (1 M = 1 mol dm^{-3}) assuming the RRS mechanism and using rotating disk electrode experiments.[15] Later, Heinze and co-workers reported on the electrochemical reaction mechanism of PCZ involving $PCZ^{\bullet+}$ and the oxidation states of the dimer in nitromethane using cyclic voltammetry.[16] In their work, the RRS mechanism was also proposed with a dimerization rate constant of 1.2 $\times$ 10^6 M^{-1} s^{-1}, while mentioning the significance of the equilibrium between PCZ and the $dimer^{2+}$ in this electrode reaction mechanism, because the oxidation potential of $PCZ^{\bullet+}$/PCZ is positive relative to that of the $dimer^{2+}$/$dimer^{\bullet+}$.[16]

However, due to the higher reactivity of $PCZ^{\bullet+}$, spectrochemical detection of $PCZ^{\bullet+}$ in AN with the electrochemical and chemical oxidation methods has not been carried out, whereas the absorption spectra of some carbazole cation radicals were observed using a laser photolysis method,[17] in polymers,[18,19] and in acidic zeolites.[20]

In the ETSF method, because short-lived cation radicals can be detected and analyzed in solution, a clear-cut analysis of the kinetics and mechanisms of $PCZ^{\bullet+}$ is presented by observing the dynamic transformation of the absorption spectra. As a result, the acceleration of the decay reaction of $PCZ^{\bullet+}$ by neutral PCZ was clearly observed, which proved that the dimerization reaction of $PCZ^{\bullet+}$ is not proceed via a simple RRC mechanism.

Experimental

In the present work, we used the tris(2,4-dibromophenyl)amine cation radical ($TDBPA^{\bullet+}$) as the reaction initiator, the details of which were described previously.[21] TDBPA (95%) was synthesized by Wako Pure Chemicals, Ltd., after receiving our special order. All measurements were carried out in AN (Wako Chemicals, dehydrated, H_2O < 50 ppm) as a solvent. The AN solution of $TDBPA^{\bullet+}$ was prepared by a batchwise electrolysis with 0.05 M tetrabutylammonium hexafluorophosphate ($TBAPF_6$, Fuluka, puriss. electrochem. grade), and used after diluting it to an appropriate concentration with AN. It was used to mix with the AN solution of PCZ to form $PCZ^{\bullet+}$. The PCZ (9-phenylcarbazole, sublimed, 99+%) was purchased from Aldrich and used as received.

For stopped-flow measurements, a rapid-scan stopped-flow spectroscopic system, RSP-601 (Unisoku Co., Ltd., Hirakata, Japan) was used. In this apparatus, a dynamic transformation of the absorption spectra can be observed with a minimized time interval of 1.0 ms after mixing the two solutions.

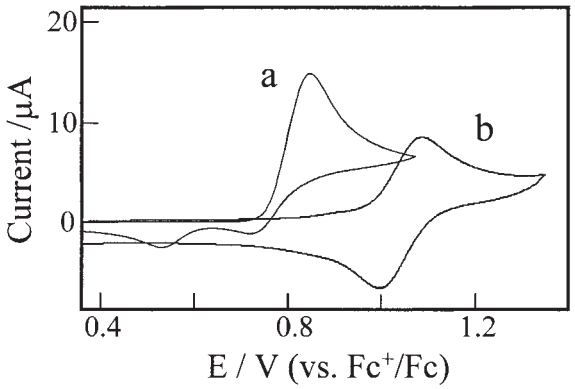

Fig. 1. Cyclic voltammograms of (a) PCZ and (b) TDBPA in AN. Working electrode; Pt disk electrode (diam. 1.6 mm). Reference electrode, Pt/(I^-,I_3^-) electrode; the potential was then converted to the value versus ferricinium ion/ferrocene (Fc^+/Fc). Scan rate; 100 mV s^{-1}. Concentration of substrate; 1.0 mM. Supporting electrolyte; 0.10 M $TBAPF_6$.

Results and Discussion

Cyclic Voltammetry. Figure 1a shows a cyclic voltammogram of 1.0 mM PCZ in AN recorded at a scan rate of 100 mV s^{-1}. From this irreversible voltammogram, which is very similar to reported ones,[16] the rapid reaction of $PCZ^{\bullet+}$ and the formation of the 3,3′-dimer can be recognized. The reduction peak at 0.53 V can be assigned to the reduction of the dimer cation radical to the dimer neutral, and the small reduction peak around 0.72 V is assigned to the reduction of the dimer dication to the dimer cation radical, as previously reported.[16]

Comparing the cyclic voltammogram of TDBPA in Fig. 1, the electron transfer reaction of Eq. 1 should be favorable in the ETSF operation, judging from the redox potential of the $TDBPA^{\bullet+}$/TDBPA couple (1.06 V vs Fc^+/Fc) and the oxidation peak potential of PCZ (0.85 V).

$$PCZ + TDBPA^{\bullet+} \rightarrow PCZ^{\bullet+} + TDBPA. \quad (1)$$

Transformation of Absorption Spectra. Thus, at first, we observed the dynamic transformation profiles of the absorption spectra by mixing an AN solution of 0.20 mM $TDBPA^{\bullet+}$ with an AN solution of 0.20 mM PCZ. Figure 2A shows the changes in the absorption spectra at a time interval of 20 ms. Just after mixing, the absorption spectrum of $TDBPA^{\bullet+}$ around 850 nm totally disappeared, which indicates a quantitative completion of Eq. 1 in the mixing section of the stopped-flow apparatus. As recognized from this figure, the absorption spectrum of $PCZ^{\bullet+}$ having absorption maxima at 720 nm and a shoulder around 650 nm could be observed explicitly, and a transformation process having two isosbestic points was observed during the course of the reaction. As for the increase of the absorbance around 430 and 930 nm, this can be attributed to the formation of the cation radical of the 3,3′-dimer, which is reasonably expected by the cyclic voltammogram in Fig. 1. In this manner, using the ETSF method, the absorption spectrum of $PCZ^{\bullet+}$

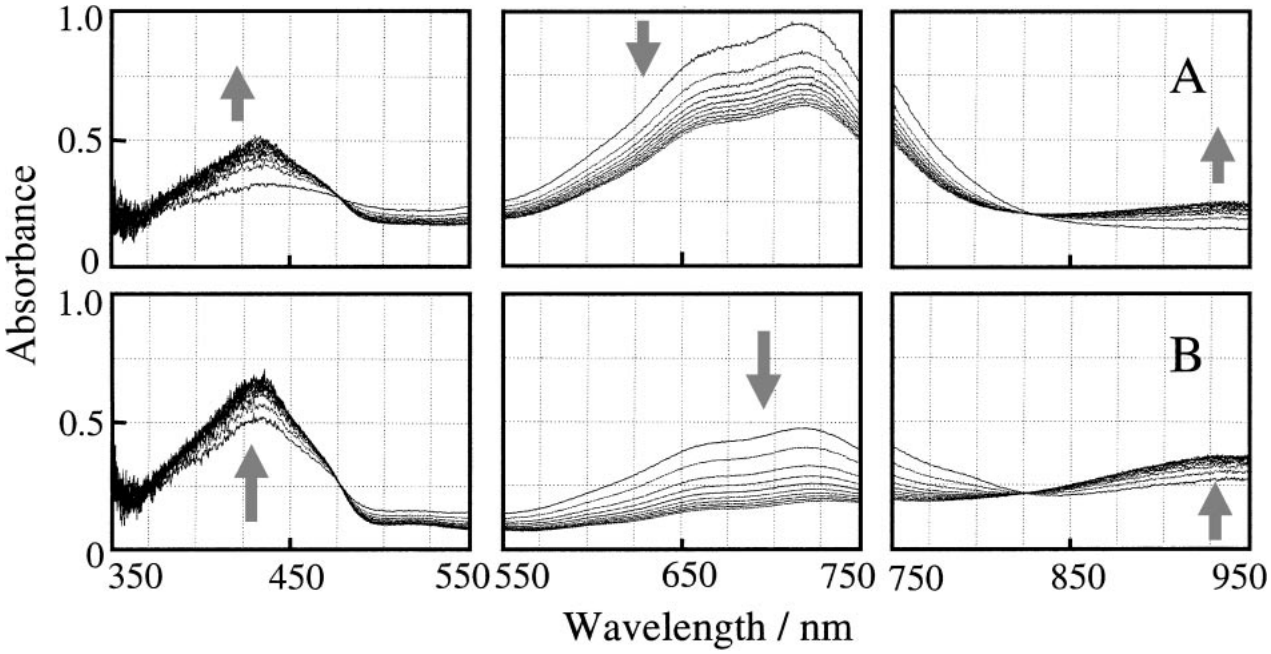

Fig. 2. (A) Dynamic transformation of absorption spectra recorded after an AN solution of 0.20 mM PCZ was mixed with an AN solution of 0.20 mM $TBPA^{\bullet+}$. Time interval of each spectrum; 20 ms. (B) Dynamic transformation of absorption spectra recorded after an AN solution of 2.0 mM PCZ was mixed with an AN solution of 0.20 mM $TBPA^{\bullet+}$. Time interval of each spectrum; 5 ms.

could be clearly observed, and the fast reaction process of $PCZ^{\bullet+}$ was followed in a time range of several tens of milliseconds.

Next, utilizing an advantage of the ETSF method, we observed the effect of neutral PCZ on the decay reaction of $PCZ^{\bullet+}$. Figure 2B shows the dynamic transformation profiles of absorption spectra by mixing the AN solution of 0.20 mM $TDBPA^{\bullet+}$ with the AN solution of 2.0 mM PCZ. The time interval of Fig. 2A was 20 ms; however, it is 5 ms in Fig. 2B. In this case, taking into account the equivolume mixing, the initial concentrations of $PCZ^{\bullet+}$ and PCZ after the mixing were 0.10 mM and 0.90 mM, respectively. Compared with the result obtained with 0.10 mM $PCZ^{\bullet+}$ without PCZ (Fig. 2A), the presence of neutral PCZ was found to accelerate the decay reaction of $PCZ^{\bullet+}$. In Fig. 2B, the acceleration is remarkable as well as the promotion of the follow-up reaction.

Reaction Mechanism of $PCZ^{\bullet+}$. Figure 3 shows the time changes in the absorbance at 720 nm, which is the absorption maximum of $PCZ^{\bullet+}$, depending on the concentration of the coexisting neutral PCZ in AN. As shown in this figure, the increase in [PCZ] brought about an increase in the decay reaction of $PCZ^{\bullet+}$. Such acceleration by the precursor molecules is quite in contrast to the reaction of $TPA^{\bullet+}$, in which the precursor molecules do not take part in the decay rate law of $TPA^{\bullet+}$. The rate law was $-d[TPA^{\bullet+}]/dt = k[TPA^{\bullet+}]^2$, and the precursor affects only the equilibrium involving the oxidation states of the dimer.[4]

To obtain the mechanistic conclusions on the acceleration by the precursor molecules, a simulation analysis was carried out for the present results of $PCZ^{\bullet+}$ (Fig. 3), assuming several expectable rate laws. For the simulation, at first, the molar absorption coefficient value, ε, has to be determined. In the present stopped-flow analysis, if the dimerization reaction of $PCZ^{\bullet+}$ proceeded after the electron transfer reaction of Eq. 1 to form

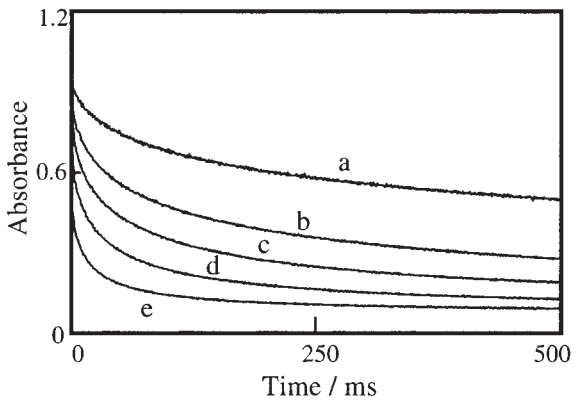

Fig. 3. Time changes in absorbance at 720 nm in the reactions of 0.10 mM $PCZ^{\bullet+}$ with (a) 0, (b) 0.10, (c) 0.20, (d) 0.40, and (e) 0.90 mM PCZ in AN.

$PCZ^{\bullet+}$ significantly before solution-stop during the dead time of ca. 1 ms, the accurate determination of ε is difficult. However, in the present case, the changes in the absorbance at 720 nm during 1 ms after stopping was ca. 1.2% under the conditions of Fig. 2A. Thus, we neglected the reaction or decrease of $PCZ^{\bullet+}$ before stopping, and estimated the ε value at 720 nm as being $1.2 \times 10^4\ M^{-1}\,cm^{-1}$ from the initial absorbance value of Fig. 2A. The ε value used in the simulation analysis therefore has a slight positive error. In addition, in the simulation analysis, the increasing component due to the formation of the dimer cation radical was added to the contribution of $[PCZ^{\bullet+}]$, as carried out previously.[4]

Consequently, a good fit was obtained with the rate law of the following equation (Fig. 4), but it was only for the decay curves in the presence of higher concentrations of PCZ (Figs. 3d and e):

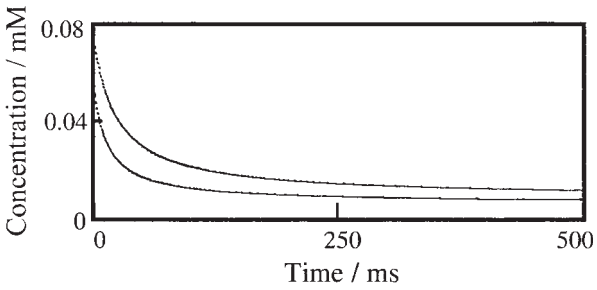

Fig. 4. Simulated results for curves (d) and (e) in Fig. 3 assuming the rate law of $-\mathrm{d[PCZ^{\bullet+}]}/\mathrm{d}t = k[\mathrm{PCZ^{\bullet+}}]^2[\mathrm{PCZ}]$ and $k = 1.4 \times 10^9\ \mathrm{M^{-2}\,s^{-1}}$. The absorbance was converted to the concentration using the molar absorption coefficient of $1.2 \times 10^4\ \mathrm{M^{-1}\,cm^{-1}}$ of $\mathrm{PCZ^{\bullet+}}$ at 720 nm.

$$-\mathrm{d[PCZ^{\bullet+}]}/\mathrm{d}t = k[\mathrm{PCZ^{\bullet+}}]^2[\mathrm{PCZ}],$$
$$k = 1.4 \times 10^9\ (\mathrm{M^{-2}\,s^{-1}}). \quad (2)$$

This mechanism indicates that the dimerization reaction proceeds via the following mechanism (Eqs. 3–6), because it is difficult to imagine the participation of PCZ in the latter step:

$$\mathrm{PCZ^{\bullet+}} + \mathrm{PCZ} \overset{K}{\rightleftarrows} (\mathrm{PCZ})_2{}^{\bullet+}, \quad (3)$$

$$(\mathrm{PCZ})_2{}^{\bullet+} + \mathrm{PCZ^{\bullet+}} \xrightarrow[\text{rds}]{k'} (\mathrm{PCZ})_2{}^{2+} + \mathrm{PCZ}, \quad (4)$$

$$(\mathrm{PCZ})_2{}^{2+} \xrightarrow[\text{fast}]{} \mathrm{Dimer} + 2\mathrm{H^+}, \quad (5)$$

$$\mathrm{Dimer} + \mathrm{PCZ^{\bullet+}} \xrightarrow[\text{fast}]{} \mathrm{Dimer^{\bullet+}} + \mathrm{PCZ}. \quad (6)$$

In the proposed mechanism, the first reaction (Eq. 3) process between $\mathrm{PCZ^{\bullet+}}$ and PCZ is in equilibrium, and the second electron-transfer process (Eq. 4) is the rate-determining step (rds). In addition, because an increase in the $\mathrm{dimer^{\bullet+}}$ and a decrease in $\mathrm{PCZ^{\bullet+}}$ were observed at the same time, the reactions of Eqs. 5 and 6 should be fast compared with the rate-determining step of Eq. 4. Based on this mechanism, the overall stoichiometry can be expressed by

$$3\mathrm{PCZ^{\bullet+}} \rightarrow \mathrm{Dimer^{\bullet+}} + \mathrm{PCZ} + 2\mathrm{H^+}. \quad (7)$$

Accordingly, Eq. 2 should be written as follows based on the stoichiometry:

$$-\mathrm{d[PCZ^{\bullet+}]}/\mathrm{d}t = 3Kk'[\mathrm{PCZ^{\bullet+}}]^2[\mathrm{PCZ}]. \quad (8)$$

Although a good fit was observed for curves (d) and (e) in Fig. 3, the fitting becomes difficult when [PCZ] becomes smaller, as in Figs. 3b and c. Furthermore, the decay curve of Fig. 3a, i.e., the decay of $\mathrm{PCZ^{\bullet+}}$ without PCZ, was very difficult to simulate based on simple rate laws, such as $-\mathrm{d[PCZ^{\bullet+}]}/\mathrm{d}t = k[\mathrm{PCZ^{\bullet+}}]^2$.

Presumably, this would be a reflection of the complexity in which the neutral PCZ takes part in the decay reaction of $\mathrm{PCZ^{\bullet+}}$, even though PCZ did not exist under the initial conditions for obtaining curve (a). Although the initial decay of $\mathrm{PCZ^{\bullet+}}$ in curve (a) might imply a direct reaction between two $\mathrm{PCZ^{\bullet+}}$s, the concentration of PCZ should increase as a consequence of the electron-transfer reaction between the formed dimer and $\mathrm{PCZ^{\bullet+}}$ (Eq. 6). Thus, a complicated mechanism is expected when the amount of PCZ is relatively small. However, the isosbestic points observed in Fig. 2A indicate that the decreased $\mathrm{PCZ^{\bullet+}}$ transferred to the dimer cation radical quantitatively follows stoichiometric relationship. In spite of such complexity, in the present results, acceleration of the reaction of $\mathrm{PCZ^{\bullet+}}$ by PCZ could be remarkably observed, and the mechanism of Eqs. 3–6 could be established.

Comparison with Electrochemical Measurements. Here, it is of interest to compare the present results in homogeneous solution with the previous results for the electrochemical oxidation of PCZ.[16] The electrode reaction mechanism of PCZ is complex because the $\mathrm{dimer^{2+}}$ is formed at the potential where PCZ is oxidized to $\mathrm{PCZ^{\bullet+}}$. Thus, the equilibrium between the $\mathrm{dimer^{2+}}$ and PCZ was previously considered to be the effect of the neutral molecule.[16] However, in the present ETSF experiment, the effect of PCZ on the decay reactions of $\mathrm{PCZ^{\bullet+}}$ could be observed explicitly, as shown in Fig. 3. From this result, it is apparent that the neutral PCZ takes part in the rate law before forming products. No $\mathrm{dimer^{2+}}$ is formed in homogeneous solution, in particular when the neutral PCZ is co-existent, because the initial ratio of $[\mathrm{PCZ^{\bullet+}}]/[\mathrm{PCZ}]$ governs the solution potential.[4]

In the present case, even though the decay reactions of $\mathrm{PCZ^{\bullet+}}$ are estimated from the voltammetric results, e.g., using a fact-scan method, the conclusion would have less meaning. This is because $\mathrm{PCZ^{\bullet+}}$ decayed even when it was formed quantitatively, as in Fig. 2A, while the neutral PCZ accelerated the decay of $\mathrm{PCZ^{\bullet+}}$ significantly. The presence of two decreasing routes should cause ambiguous results in an estimation based on the electrochemical results.

Concerning the mechanistic issues of cation radicals, conclusions for the cases of RSC mechanism would be somewhat difficult to obtain, even though the previous studies revealed an interaction with the parent molecules.[5–7] This is because, e.g., in the present case, the formation of the $\mathrm{dimer^{\bullet+}}$ in Eq. 6 can occur via electron transfer from the electrode (and furthermore, $\mathrm{dimer^{\bullet+}}$ can be oxidized to $\mathrm{dimer^{2+}}$ on the electrode). However, in the ETSF method, a clear-cut analysis can be performed by eliminating the possibility of electrode reaction processes of the products, as in the present paper. The ETSF analysis is thus effective in revealing the electrochemical events by focusing on homogeneous reactions involving electrogenerated species.

Conclusions

In conclusion, in the present work, the dynamic transformation of the absorption spectra of $\mathrm{PCZ^{\bullet+}}$ could be observed in AN for the first time using the ETSF method, though the absorption spectra of electrogenerated carbazole cation radicals were recorded only for specific derivatives, e.g., having blocking substituents on the 3, 6 positions.[15] Although the ETSF method was valid for observations of the absorption spectra of the anthracene derivative cation radicals,[21] the present case is also a good example showing the ability of the ETSF method for the detection of short-lived cation radicals.

In addition, the acceleration of the dimerization reaction of $\mathrm{PCZ^{\bullet+}}$ in the presence of neutral PCZ was clearly demonstrated from the changes in the dynamic transformation of the absorption spectra. From the decay curves of $\mathrm{PCZ^{\bullet+}}$, the reaction mechanism of Eqs. 3–6 could be proposed for the dimerization

of $PCZ^{\bullet+}$, in spite of the complicated decay process when $PCZ^{\bullet+}$ was formed without PCZ. Nevertheless, the isosbestic points observed in Fig. 2 indicate the simple and rapid transformation route from $PCZ^{\bullet+}$ to the 3,3′-$dimer^{\bullet+}$, which verifies the fast follow-up reactions after the rate-determining step.

As for the differences between $PCZ^{\bullet+}$ and $TPA^{\bullet+}$, the mechanistic change should be stressed in addition to changes in the known reactivity.[15] To clarify the differences, we are now analyzing the dimerization reactions of 9-(*p*-substituted-phenyl)-carbazole cation radicals.

This work was supported in part by a Grant-in-Aid for Scientific Research from the Ministry of Education, Culture, Sports, Science and Technology, No. 13640602.

References

1 M. Schmittel and A. Burghart, *Angew. Chem., Int. Ed. Engl.*, **36**, 2550 (1997).

2 H. G. Yang and A. J. Bard, *J. Electroanal. Chem.*, **304**, 87 (1991).

3 D. Larumbe, I. Gallardo, and C. P. Andrieux, *J. Electroanal. Chem.*, **304**, 241 (1991).

4 M. Oyama, T. Higuchi, and S. Okazaki, *J. Chem. Soc., Perkin Trans. 2*, **2001**, 1287.

5 B. Aalstad, A. Ronlan, and V. D. Parker, *Acta Chim. Scand.*, **B35**, 247 (1981).

6 C. L. Kulkarni, B. J. Scheer, and J. F. Rusling, *J. Electroanal. Chem.*, **140**, 54 (1982).

7 K. Nozaki, M. Oyama, H. Hatano, and S. Okazaki, *J. Electroanal. Chem.*, **270**, 191 (1989).

8 M. Oyama, T. Higuchi, and S. Okazaki, *Electrochem. Commun.*, **2**, 675 (2000).

9 M. Oyama and T. Higuchi, *J. Electrochem. Soc.*, **149**, E12 (2002).

10 M. Oyama, M. Goto, and H. Park, *Electrochem. Commun.*, **4**, 110 (2002).

11 M. Goto, H. Park, K. Otsuka, and M. Oyama, *J. Phys. Chem. A*, **106**, 8103 (2002).

12 M. Oyama, T. Higuchi, and S. Okazaki, *Electrochem. Commun.*, **3**, 363 (2001).

13 N. V. Rees, O. V. Klymenko, R. G. Compton, and M. Oyama, *J. Electroanal. Chem.*, **531**, 33 (2002).

14 J. F. Ambrose and R. F. Nelson, *J. Electrochem. Soc.*, **115**, 1159 (1968).

15 J. F. Ambrose, L. L. Carpenter, and R. F. Nelson, *J. Electrochem. Soc.*, **122**, 876 (1975).

16 J. Heinze, K. Hinkelmann, M. Dietrich, and J. Mortensen, *Ber. Bunsenges. Phys. Chem.*, **89**, 1225 (1985).

17 H. Masuhara, N. Tamai, N. Mataga, F. C. Schryver, and J. Vandendriessche, *J. Am. Chem. Soc.*, **105**, 7256 (1983).

18 H. Masuhara, K. Yamamoto, N. Tamai, K. Inoue, and N. Mataga, *J. Phys. Chem.*, **88**, 3971 (1984).

19 Y. Tsujii, A. Tsuchida, Y. Onogi, and M. Yamamoto, *Macromolecules*, **23**, 4019 (1990).

20 H. Garcia, V. Marti, I. Casades, V. Fornes, and H. D. Roth, *Phys. Chem. Chem. Phys.*, **3**, 2955 (2001).

21 M. Oyama, J. Matsui, and H. Park, *Chem. Commun.*, **2002**, 604.